Hadronic B Decays at LHCb

C.R. Jones

HEP Group, Cavendish Laboratory, JJ Thomson Avenue, Cambridge, CB3 0HE. United Kingdom

The article outlines three new or updated LHCb[1] results[2,3,4] presented at Moriond QCD 2012, using $1.0\,\mathrm{fb}^{-1}$ of data collected in 2011.

1 $\overline{B}{}^0_s$ to double-charm final states

Double charm decays of B mesons provide an interesting avenue to search for signs of new physics beyond the Standard Model (SM). For example, the decays $\overline{B}{}^0 \to D^+D^-$ and $\overline{B}{}^0_s \to D^+_s D^-_s$ can be used to measure the weak phase γ, assuming U-spin symmetry and the decay $\overline{B}{}^0 \to D^+D^-$ provides an alternate way to measure $\sin(2\beta)$, which can in principle differ from the values determined in $\overline{B}{}^0 \to (c\overline{c})K^0_{\mathrm{S}}$ because of penguin contributions.

1.1 Event Selection and Analysis

Signal candidates are formed using reconstructed $D^0 \to K^-\pi^+$, $D^+ \to K^-\pi^+\pi^+$ and $D^+_s \to K^+K^-\pi^+$ decays[2]. The B candidates are then reconstructed from the appropriate pair of charm mesons, applying both mass and vertex constraints to the assumed decay chain and loose particle identification requirements on the D children. To further improve the signal purity, a multi-variate selection is then applied, trained on data using clean signals of D mesons obtained from background subtracted $\overline{B}{}^0_{(s)} \to D^+_{(s)}\pi^-$ and $B^- \to D^0\pi^-$ decays. Background for the training is taken from the D mass sideband regions. In addition to including kinematical quantities of the D and the D children, a number of track-quality and particle-identification variables are also used to maximize the discriminating power.

The mass spectra are fitted using a single Crystal Ball function which is used for all $\overline{B} \to D\overline{D}'$ modes. Simulated events are used to derive Gaussian parametrizations for the backgrounds due to mis-reconstructed decays. An exponential combinatoric background term is also included. Examples of the fitted mass spectra are shown in Figures 1 and 2.

The results for the branching ratios, computed from the fitted signal yields, are

$$\begin{aligned}
&\frac{\mathcal{B}(\overline{B}{}^0_s \to D^+D^-)}{\mathcal{B}(\overline{B}{}^0 \to D^+D^-)} = 1.00 \pm 0.18 \pm 0.09 \quad , &&\frac{\mathcal{B}(\overline{B}{}^0_s \to D^+_s D^-)}{\mathcal{B}(B^0 \to D^+_s D^-)} = 0.048 \pm 0.008 \pm 0.004, \\
&\frac{\mathcal{B}(\overline{B}{}^0_s \to D^+_s D^-_s)}{\mathcal{B}(\overline{B}{}^0 \to D^+ D^-_s)} = 0.508 \pm 0.026 \pm 0.043, &&\frac{\mathcal{B}(\overline{B}{}^0_s \to D^0 \overline{D}{}^0)}{\mathcal{B}(B^- \to D^0 D^-_s)} = 0.015 \pm 0.004 \pm 0.002,
\end{aligned} \tag{1}$$

where the errors are statistical and systematic respectively. See[2] for details on the determination of the systematic uncertainities.

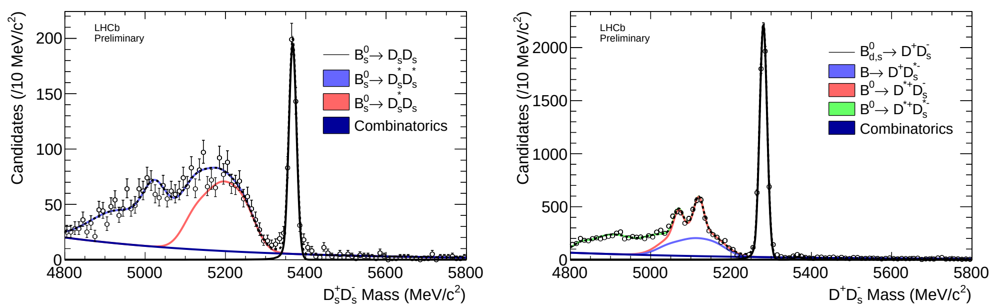

Figure 1: Invariant mass distributions for $\overline{B}{}^0_s \to D_s^+ D_s^-$ (left) and $\overline{B}{}^0 \to D^+ D_s^-$ (right) candidates.

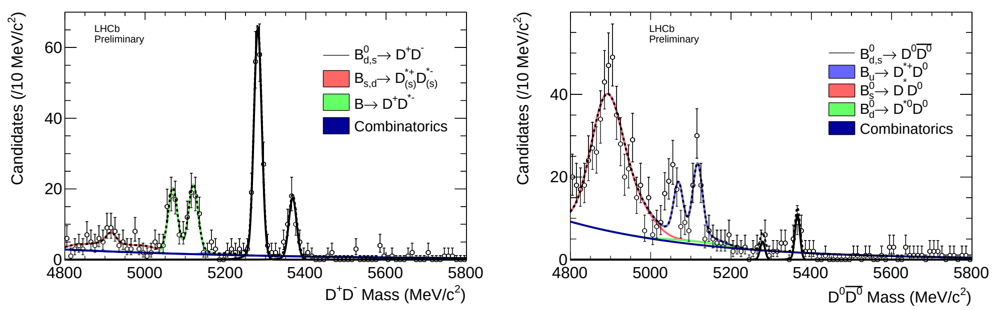

Figure 2: Invariant mass distributions for $\overline{B}{}^0_{(s)} \to D^+ D^-$ (left) and $\overline{B}{}^0_{(s)} \to D^0 \overline{D}{}^0$ (right).

1.2 Summary

First observations and relative branching fractions measurements of the decays $\overline{B}{}^0_s \to D^+D^-$, $\overline{B}{}^0_s \to D_s^+ D^-$ and $\overline{B}{}^0_s \to D^0 \overline{D}{}^0$ have been made [2]. A new result on the branching fraction of $\overline{B}{}^0_s \to D_s^+ D_s^-$ relative to $\overline{B}{}^0_s \to D_s^+ D^-$, which has a precision about 5 times better than the current world average value [5] has also been presented.

2 Observation of CP violation in $B^\pm \to DK^\pm$ decays

Testing the unitary of the CKM quark mixing matrix, by verifing the condition $V_{ud}V_{ub}^* + V_{cd}V_{cb}^* + V_{td}V_{tb}^* = 0$, is a powerful check of the SM. This condition describes a triangle in the complex plane, whose area is proportional to the amount of CP violation in the model, and the unitary of which can be tested by making over-constraining measurements of its sides and angles.

Measurements of the partial widths of $B^\pm \to DK^\pm$ decays, with D either a D^0 or $\overline{D}{}^0$ meson, provide one of the most powerful methods for determining the currently least-well determined observable, the CKM phase $\gamma = \arg\left(-V_{ud}V_{ub}^*/V_{cd}V_{cb}^*\right)$. If the same D final state is accessible for both D^0 and $\overline{D}{}^0$ mesons, the interference of these two processes gives sensitivity to γ and may exhibit direct CP violation. This feature of open-charm B^- decays was first recognised in its application to CP eigenstates, such as $D \to K^+K^-$, $\pi^+\pi^-$ [6,7] but can be extended to other decays, *e.g.* $D \to \pi^- K^+$, labelled "ADS" modes in reference to the authors [8,9].

2.1 Event Selection and Analysis

All sixteen combinations of $B^\pm \to Dh^\pm$, $D \to h^\pm h^\mp$ with $h = K, \pi$ are formed with the candidate D mass within $1765 - 1965$ MeV/c^2. P and Pt cuts are applied to the D daughter tracks, in order to ensure best pion versus kaon discrimination.

A multi-variate selection is then trained using a simulated sample of $B^\pm \to [K^\pm\pi^\mp]_D K^\pm$ and background events from the D sideband ($35 < |m(hh) - m_{\rm PDG}^{D^0}| < 100$ MeV/c^2) of an independent sample collected in 2010. The selection uses a combination of track and vertex quality variables, $B^\pm$ and D flight distance and the angle between the $B^\pm$ momentum vector and the line joining its decay vertex to the primary interaction vertex. For futher details see [3].

The observables of interest are determined from a fit to the invariant mass distributions of selected B candidates, as shown in Figure 3.

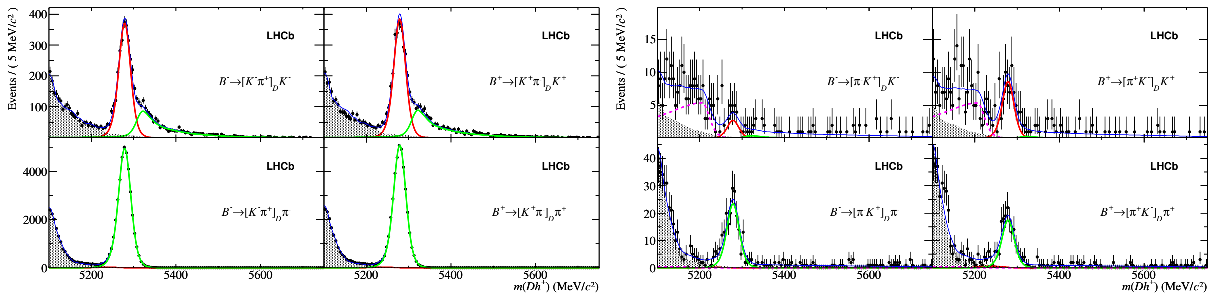

Figure 3: Invariant mass distributions of $B^\pm \to [K^\pm\pi^\mp]_D h^\pm$ (left) and $B^\pm \to [\pi^\pm K^\mp]_D h^\pm$ (right) candidates.

In total, thirteen observables are measured in the fit:

$$R^f_{K/\pi} = \frac{\Gamma(B^- \to [f]_D K^-) + \Gamma(B^+ \to [f]_D K^+)}{\Gamma(B^- \to [f]_D \pi^-) + \Gamma(B^+ \to [f]_D \pi^+)}, \qquad R^\pm_h = \frac{\Gamma(B^\pm \to [\pi^\pm K^\mp]_D h^\pm)}{\Gamma(B^\pm \to [K^\pm \pi^\mp]_D h^\pm)}$$
$$A^f_h = \frac{\Gamma(B^- \to [f]_D h^-) - \Gamma(B^+ \to [f]_D h^+)}{\Gamma(B^- \to [f]_D h^-) + \Gamma(B^+ \to [f]_D h^+)} \tag{2}$$

where f represents KK, $\pi\pi$ and the favoured $K\pi$ mode. The following quantities are deduced:

$$\begin{aligned}
R_{CP+} \approx \; < R^{KK}_{K/\pi}, R^{\pi\pi}_{K/\pi} > / R^{K\pi}_{K/\pi} &= 1.007 \pm 0.038(\text{stat}) \pm 0.012(\text{syst}) \\
A_{CP+} = \; < A^{KK}_K, A^{\pi\pi}_K > &= 0.145 \pm 0.032(\text{stat}) \pm 0.010(\text{syst}) \\
R_{\text{ADS}(K)} = (R^-_K + R^+_K)/2 &= 0.0152 \pm 0.0020(\text{stat}) \pm 0.0004(\text{syst}) \\
A_{\text{ADS}(K)} = (R^-_K - R^+_K)/(R^-_K + R^+_K) &= -0.52 \pm 0.15(\text{stat}) \pm 0.02(\text{syst}) \\
R_{\text{ADS}(\pi)} = (R^-_\pi + R^+_\pi)/2 &= 0.00410 \pm 0.00025(\text{stat}) \pm 0.00005(\text{syst}) \\
A_{\text{ADS}(\pi)} = (R^-_\pi - R^+_\pi)/(R^-_\pi + R^+_\pi) &= 0.143 \pm 0.062(\text{stat}) \pm 0.011(\text{syst}),
\end{aligned}$$

2.2 Summary

The $B^\pm \to DK^\pm$ ADS mode has been observed with a statistical significance of $\sim 10\sigma$ and displays evidence (4.0σ) of a large negative asymmetry. The $B^\pm \to D\pi^\pm$ ADS mode shows a hint of a positive asymmetry with 2.4σ significance. The KK and $\pi\pi$ modes both show positive asymmetries. The statistical significance of the combined asymmetry, A_{CP+}, is 4.5σ. With a total significance of 5.8σ, direct *CP* violation in $B^\pm \to DK^\pm$ decays is observed.

3 Polarization amplitudes and triple product asymmetries in the decay $B^0_s \to \phi\phi$

In the SM, the flavour-changing neutral current decay $B^0_s \to \phi\phi$ proceeds via a $b \to s\bar{s}s$ penguin process. These decays can be used to investigate new sources of CP violation in the comparison of their time-dependent CP asymmetry with the charmonia modes (e.g $B_s \to J/\Psi\phi$).

As the decay is a pseudoscalar to vector-vector transition, three possible spin configurations of the vector meson pair are allowed by angular momentum conservation, namely H_{+1}, H_{-1} and H_0. From these states, three linear polarization amplitudes can be defined

$$A_0 = H_0\,, \qquad A_\perp = \frac{H_{+1} - H_{-1}}{\sqrt{2}}\,, \qquad A_\parallel = \frac{H_{+1} + H_{-1}}{\sqrt{2}}\,. \tag{3}$$

The $\phi\phi$ final state can be a mixture of *CP*-even and *CP*-odd eigenstates. The longitudinal (A_0) and parallel ($A_\parallel$) components are *CP*-even and the perpendicular component ($A_\perp$) is

CP-odd. From the V–A structure of the weak interaction, the longitudinal component, $f_L = |A_0|^2/(|A_0|^2 + |A_\perp|^2 + |A_\parallel|^2)$, is expected to be dominant. The revelant decay angles are defined in Figure 4 .

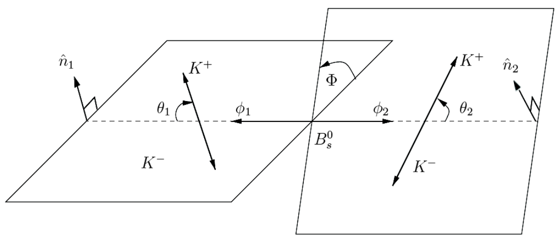

Figure 4: Decay angles for the $B_s^0 \to \phi\phi$ decay.

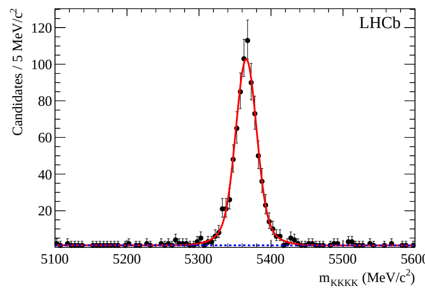

Figure 5: Invariant $K^+K^-K^+K^-$ mass distribution.

A search for physics beyond the SM can also be performed by studying the triple products $U = \sin(2\Phi)/2$ and $V = \pm\sin(\Phi)$. Non zero values of the asymmetries in these variables (0 in the SM), A_U and A_V, can be either due to *T*-violation or final-state interactions.

3.1 Event Selection and Analysis

$B_s^0 \to \phi\phi$ candidates are reconstructed[4] using events where both ϕ mesons decay into a K^+K^- pair. Excellent signal purity (Figure 5) is achieved using cuts on the minimum impact parameter of the tracks to all reconstructed *pp* interaction vertices, and by requiring the tracks also are identified as kaons.

3.2 Summary

The polarization amplitudes ($|A_0|^2$, $|A_\perp|^2$, $|A_\parallel|^2$) and triple product asymetries A_U and A_V are determined by performing an unbinned maximum likelihood fits to data. The results are :-

$$\begin{aligned}
|A_0|^2 &= 0.365 \pm 0.022\,(\text{stat}) \pm 0.012\,(\text{syst})\,, \\
|A_\perp|^2 &= 0.291 \pm 0.024\,(\text{stat}) \pm 0.010\,(\text{syst})\,, \\
|A_\parallel|^2 &= 0.344 \pm 0.024\,(\text{stat}) \pm 0.014\,(\text{syst})\,, \\
\cos(\delta_\parallel) &= -0.844 \pm 0.068\,(\text{stat}) \pm 0.029\,(\text{syst})\,.
\end{aligned}
\qquad
\begin{aligned}
A_U &= -0.055 \pm 0.036\,(\text{stat}) \pm 0.018\,(\text{syst})\,, \\
A_V &= 0.010 \pm 0.036\,(\text{stat}) \pm 0.018\,(\text{syst})\,.
\end{aligned}$$

and are consistent previous measurements and do not exhibit any T-odd violation effects.

1. A.Augusto Alves et al. The LHCb Detector at the LHC. *JINST*, 3:S08005, 2008.
2. First observations and branching fraction measurements of $\overline{B}_s^0$ to double-charm final states LHCb-CONF-2012-009.
3. Observation of *CP* violation in $B^\pm \to DK^\pm$ decays LHCb-PAPER-2012-001.
4. Measurement of the polarization amplitudes and triple product asymmetries in the $B_s^0 \to \phi\phi$ decay LHCb-PAPER-2012-004.
5. K. Nakamura et al. Review of particle physics. *J. Phys.*, G37:075021, 2010.
6. Michael Gronau and David London. How to determine all the angles of the unitarity triangle from $B_d^0 \to DK_S^0$ and $B_s^0 \to D\phi$. *Phys. Lett.*, B253:483, 1991.
7. Michael Gronau and Daniel Wyler. On determining a weak phase from *CP* asymmetries in charged B decays. *Phys. Lett.*, B265:172, 1991.
8. David Atwood, Isard Dunietz, and Amarjit Soni. Enhanced CP violation with $B \to KD^0(\overline{D}^0)$ modes and extraction of the CKM angle γ. *Phys.Rev.Lett.*, 78:3257, 1997.
9. David Atwood, Isard Dunietz, and Amarjit Soni. Improved methods for observing CP violation in $B^\pm \to KD$ and measuring the CKM phase γ. *Phys.Rev.*, D63:036005, 2001.